A flow and transport model for low-temperature gaseous nitrocarburizing of stainless steels

J. Feng[1,*], S. Lohrei[1], M. Wettlaufer[1,**]
[1]Centre of Materials Engineering, Heilbronn University, Max-Planck-Str. 39, DE-74081 Heilbronn, Germany
[1,*]jian.feng@hs-heilbronn.de; [1,**]marc.wettlaufer@hs-heilbronn.de

Abstract: Stainless steels were nitrocarburized at low temperatures in an industrial furnace built for thermochemical treatments. An integrated numeric, thermodynamic, and experimental analysis work was conducted to find out the proper flow and transport parameters of combined chemical species, which were responsible for a steady thermochemical atmosphere essential for the antipassivation of the surface of stainless steels. A flow and transport model was built to solve fluid flow, heat transfer and mass transport during the purge and pulse cycles. The simulated results were confirmed by experimental measurements. It has been concluded that numeric simulation can assist the design of industrial thermochemical treatments to effectively remove the passive layer of stainless steels.

Keywords: flow, transport, nitrocarburizing, gaseous, stainless steels.

1. Introduction

Low temperature nitrocarburizing is a promising treatment to improve the wear resistance and load bearing capacity of austenitic stainless steels (ASS) without deteriorating the corrosion performance [1-2]. Low temperature gaseous thermochemical treatment enables straightforward thermodynamic definition as regards process parameters and controlled formation of the case on the complexly structured workpieces, which is attractive for the industrial applications [2]. By inheriting all the advantages and characteristics of double layers, i.e. the nitrogen- and carbon-rich expanded austenite, a gradual change in mechanical properties between the nitrocarburized case and ASS core can be achieved [3]. The corrosion resistance of ASS arises from a dense chromium-rich oxide layer that forms naturally and prevents diffusion of interstitial species into the base materials. In order to remove the passive layer, required gaseous partial pressures of acetylene and hydrogen gas are calculated thermodynamically. The obtained data will be coupled with purge and pulse cycles numerically simulated with COMSOL Multiphysics®. Thus, applicable processing parameters can be determined.

2. Thermodynamic Calculations

During the purge and pulse cycles, following gaseous chemical species NH_3, C_2H_2, H_2, N_2, a small amount of O_2 and H_2O coexist in the furnace cell. Generally, chemical reactions take place on the surface of the samples and barely in the gaseous atmosphere. It is the ratio of gaseous partial pressure that controls the antipassivation. The partial pressures of various Cr-based gaseous species are plotted in Figure 1 as a function of the oxygen partial pressure at a given temperature of 673 K. $P_{C_2H_2}/P_{H_2}$ should be greater than P_{crit} to access the antipassivation. For any given Cr-based gaseous species, this functional relation can be calculated from the thermodynamic equilibrium between the relevant Cr-based solid and gaseous species. The utilized equations are listed below:

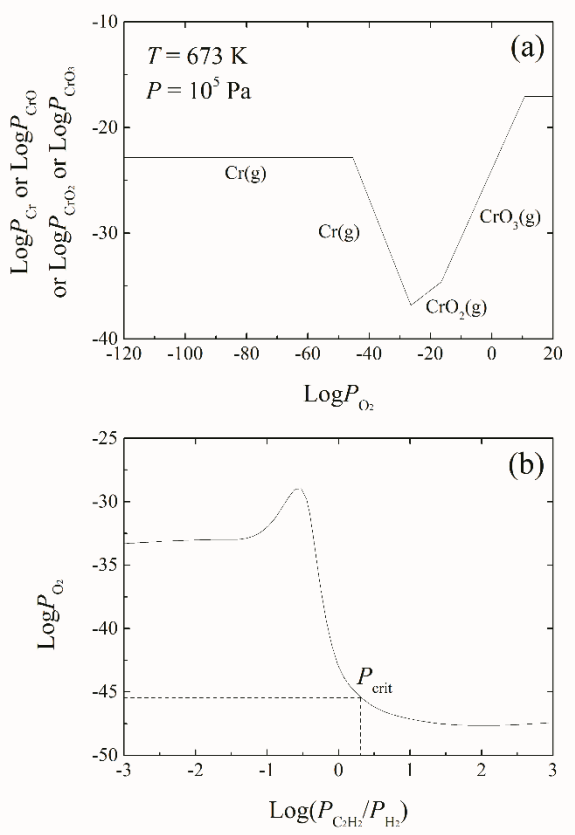

Figure 1. Calculated boundary conditions.

$$\Delta H(T) = \left(\Delta H^{O}_{f\mathrm{Cr_2O_3}} + \int_{298.15}^{T} C_{\mathrm{PCr_2O_3}}(T)dT\right) - 2\left(\Delta H^{O}_{f\mathrm{Cr}} + \int_{298.15}^{T} C_{\mathrm{PCr}}(T)dT\right) - \frac{3}{2}\left(\Delta H^{O}_{f\mathrm{O_2}} + \int_{298.15}^{T} C_{\mathrm{PO_2}}(T)dT\right)$$

$$\Delta S(T) = \left(\Delta S^{O}_{f\mathrm{Cr_2O_3}} + \int_{298.15}^{T} \frac{C_{\mathrm{PCr_2O_3}}(T)}{T}dT\right) - 2\left(\Delta S^{O}_{f\mathrm{Cr}} + \int_{298.15}^{T} \frac{C_{\mathrm{PCr}}(T)}{T}dT\right) - \frac{3}{2}\left(\Delta S^{O}_{f\mathrm{O_2}} + \int_{298.15}^{T} \frac{C_{\mathrm{PO_2}}(T)}{T}dT\right)$$

$$\Delta G(T) = \Delta H(T) - T\Delta S(T) = -2.303RT\log K(T)$$

3. Use of COMSOL Multiphysics

The fluid flow, heat Transfer, and mass transport in nitrocarburization is modeled with COMSOL Multiphysics 5.2a. The related differential equations found in [4] are briefly explained below. The mass transport in reacting systems where fluid flow is modeled with the convection-diffusion equation

$$\frac{\partial c}{\partial t} + \nabla \cdot (-D\nabla c) + \boldsymbol{u} \cdot \nabla c = R_i$$

In the mass transport, the concentrations at the inlet are fixed. At the outlet, the convection or alternatively a defined vacuum pump dominates. The general heat transfer in time-dependent studies is governed by

$$\rho C_P \left(\frac{\partial T}{\partial t} + \boldsymbol{u} \cdot \nabla T\right) = \nabla \cdot (\kappa \nabla T)$$

whereas in the stationary studies by the advection. The laminar flow is described by Navier-Stokes equations and the continuity equation

$$\rho\left(\frac{\partial \boldsymbol{u}}{\partial t} + \boldsymbol{u} \cdot \nabla \boldsymbol{u}\right) = -\nabla p + \nabla \cdot \left(\mu(\nabla \boldsymbol{u} + (\nabla \boldsymbol{u})^T)\right)$$

$$\nabla \cdot \boldsymbol{u} = 0$$

The Brinkman equations and the continuity equation are applied to the reaction unit in the middle of the cell. These equations are implemented with COMSOL Multiphysics® in a 3D model. Because of symmetry, only one-half of the reactor is modeled. Meshes are created based on mapped structures. In all interfaces, discretization is set to default conditions. The initial and boundary conditions to solve these equations are given by experimental inlet conditions and a given outlet pressure of 1 atm.

4. Simulation results

Figure 2 shows the calculation results for the magnitude of the velocity field in the cell. The cell temperature was 673 K and the flow was studied stationarily. The gas inlet was on the top of the cell connected with a gas supply. The static mixer on the left side of the cell adopted constant speed. Before the antipassivation begins, the cell was defined to be evacuated till 10^{-4} bar and then filled with H_2 of 1 mol/m^3. From the results, it can be seen that the velocity magnitude of gas flow in the upper part of the reaction unit is relatively low. Figure 3 shows the pressure drop, which occurs mainly across the reaction unit. The pressure decays very rapidly with the distance from the nozzle.

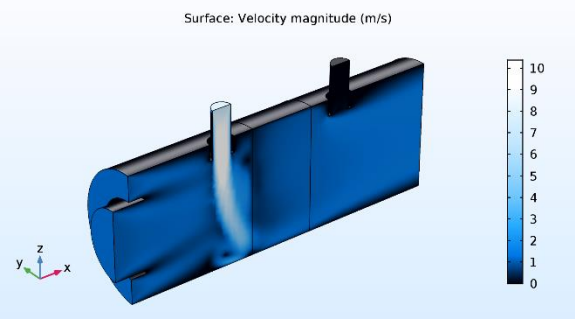

Figure 2. The magnitude of the velocity field in the cell.

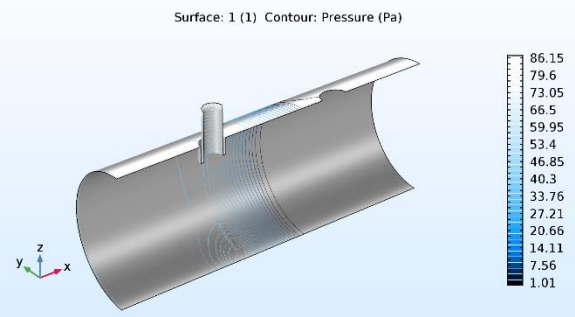

Figure 3. Pressure contour in the cell.

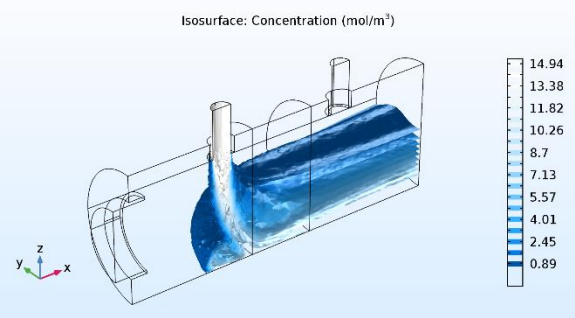

Figure 4. Isoconcentration surfaces for C_2H_2.

Isoconcentration surfaces for C_2H_2 and H_2 are shown in Figure 4 and Figure 5, respectively. As a result, the ratio of gaseous partial pressure $P_{C_2H_2}/P_{H_2}$ can be calculated from the general gas equation in each location in both the reaction unit and rest space of the cell. The modelled concentrations of H_2 are then compared with measured values obtained from a H_2 sensor placed inside the cell. In conclusion, the model shows that the static mixer should adopt a higher speed. The reactants were not sufficiently mixed and only a fraction of the reaction unit is utilized.

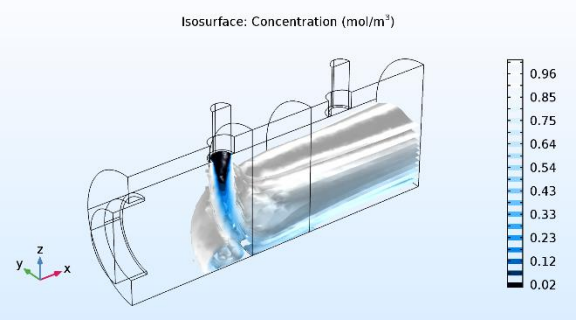

Figure 5. Isoconcentration surfaces for H_2.

5. Conclusions

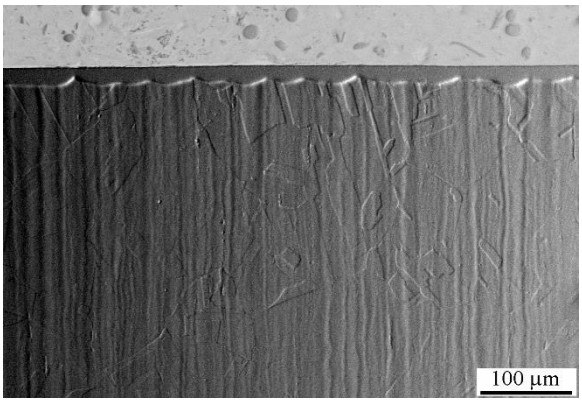

Figure 6. Nitrocarburized AISI 303 ASS.

In summary, COMSOL Multiphysics® is a powerful tool to understand thermochemical processes in the heat treatment industry. With simple physical modules, fluid flow and transport inside the furnace cell can be evaluated. The purge and pulse cycles can be better understood and controlled. The applicable process parameters can be easily converted from thermodynamic calculations. With these converted parameters, clean and fine constructed nitrocarburized layers consisting of expanded austenite were successfully obtained (Figure 6). Therefore, it is concluded that numeric simulation with the posted flow and transport model can greatly assist the industrial thermochemical treatments and effectively remove the passive layer of stainless steels.

6. References

1. T. Bell, Y. Sun, and A. Suhadi, Environmental and technical aspects of plasma nitrocarburizing, *Vacuum* **59**(1), 14-23 (2000).
2. T. Christiansen, M. A. Somers, Low-temperature gaseous nitriding and carburizing of stainless steel, *Surface Engineering*, **21**(5-6), 445-455 (2005).
3. C. Dawes, Nitrocarburizing and its influence on design in the automotive sector, *Surface Engineering* **7**(1), 29-44 (1991).
4. Chemical Reaction Engineering Module User's Guide, Version 5.2a, COMSOL AB, 2016

7. Acknowledgements

This work was sponsored by the AiF under the ZIM program, grant No. KF 2126912KM4. The authors acknowledge the support and partnership from J. Reese, Härterei Reese Brackenheim, and N. Vucemilovic, KGO.

8. Nomenclature

c	molar concentration, mol/m^3
C_p	specific heat capacity, J/(kg·K)
D	applied diffusivity, m^2/s
ΔG	Gibbs free energy, J
ΔH	enthalpy, J
K	equilibrium constant
κ	thermal conductivity, W/(m·K)
μ	gas dynamic viscosity, Pa·s
p	gas pressure, Pa
R	gas constant, J/(mol·K)
R_i	reaction rate for species i, mol/(m^3·s)
ΔS	entropy, J/K
T	temperature, K
$\boldsymbol{u}$	gas velocity vector, m/s
ρ	specific density, kg/m^3